SANDIA REPORT SAND83—1506 • Unlimited Release • UC—38
Printed September 1983

SAND--83-1506
DE84 002052

Tape Joint Design Guidelines

Robert P. Rechard, Joseph T. Black, Jr., Stanley D. Meyer

Prepared by
Sandia National Laboratories
Albuquerque, New Mexico 87185 and Livermore, California 94550
for the United States Department of Energy
under Contract DE-AC04-76DP00789

Issued by Sandia National Laboratories, operated for the United States Department of Energy by Sandia Corporation.

Printed in the United States of America
Available from
National Technical Information Service
U.S. Department of Commerce
5285 Port Royal Road
Springfield, VA 22161

NTIS price codes
Printed copy: A03
Microfiche copy: A01

SAND83–1506
Unlimited Release
Printed September 1983

Distribution
Category UC–38

Tape Joint Design Guidelines

Robert P. Rechard
Joseph T. Black, Jr.
Stanley D. Meyer
Engineering Analysis Department 1520
Sandia National Laboratories
Albuquerque, NM 87185

Abstract

Connections joining cylindrical cases are required in applications ranging from pipelines to rocket bodies. The tape joint exceeds in versatility most other joints in these applications. It is strong in both bending and axial loading; easy to design, analyze, fabricate, and assemble; and space-efficient and lightweight. The vital features of the tape joint (interlocking tabs and offset tape grooves) and the assembly procedure are discussed. Important dimensions (tape groove depth, area above and below the tape tunnel, length separating tape tunnel and interlocking tabs, and throat length) and specifications necessary for the ensured success of the joint are explained. A 12-step design procedure follows in a separate, easily referenced section. Finally, application examples are presented that show the details associated with tolerancing. Examples of possible modifications also are shown to demonstrate the versatility of the tape joint.

Contents

Figures

Summary

Connections joining axisymmetric, thin-shelled cases are required in applications ranging from pipelines and ovate culverts to rocket bodies. The tape joint, first patented in 1971, supersedes in versatility most other joints in these applications. It is stiff and strong in both bending and axial loading; easy to design, analyze, fabricate, and assemble; and space-efficient and lightweight.

The components of the tape joint are the mating inner and outer built-up coupling, each with an interlocking tab and tape groove. The interlocking tabs help align the joint and prevent excessive deformation when the joint is loaded axially or with a bending moment. The grooves form a tape tunnel in which two tapes are inserted. Slight misalignment of the grooves allows the the tape segments to wedge the joint tightly closed. The tape segments are slotted to facilitate insertion. Access to the tunnel is usually through two access slots cut 180° apart.

Projects in the intervening years since inception have provided experience sufficient to establish a design procedure. Designing the joint involves:

- Calculating the optimum net tensile thickness (T), groove height (h), and radius values R_5, R_4, R_3, R_2, and R_1.
- Evaluating the axial dimensions, such as the tunnel separation length (ℓ), tape pair width (w), tape tunnel width (W), and throat length (L).
- Calculating the tape dimensions [tape length (x), minimum tape slit width (a), and minimum hinge depth (d)] and the tape slot length (y).

The above steps are presented in a separate, easily referenced section in the text.

Minimizing the joint radial thickness was the primary performance criterion used to dimension the joint. Secondary criteria were ease of fabrication and assembly, minimizing weight, and cost considerations. An important constraint was that joint strength exceeds the structural shell strength.

In order to use the joint's versatility, it is necessary to understand the purpose of the tape joint features; then sensible modifications can be made. (For example, the interlocking tabs permit the joint to withstand high-bending forces. Extending the shells well beyond the tape tunnel can be used as an alternate feature, as demonstrated in the text.) Understanding the tape joint features also ensures success in normal applications; for example, knowledge of the most critical dimensions(R_3, ℓ), the location of the tape groove, and that only one point of closure should be specified permits much looser tolerancing on other dimensions. This, in turn, results in cost reductions for the joint.

Nomenclature

a	Tape slit width
b	Tape height
D	Individual tape width dimension
d	Tape hinge depth
F_{bru}	Ultimate bearing strength
F_{su}	Ultimate shear strength
F_{tu}	Ultimate tensile strength
H	Tape tunnel height
h	Tape groove height
h_s	Additional tape tunnel spacing caused by straight tape segments
K_t	Stress concentration factor
L	Throat length: length between start of enlarged cylinder thickness and interlocking tab
ℓ	Tunnel separation length: length between tape tunnel and interlocking tab (equal to the reciprocal of the shell characteristic λ)
m	Joint upset thickness
n	Number of segments of length p
p	Tape slit pitch (spacing)
R	Radius from body or pipe centerline
r	Tape groove corner radius
s	Arc length of access hole
T	Net tensile section thickness
t	Structural material shell thickness
W	Tape tunnel width
w	Tape pair width
x	Tape length
y	Linear length of access hole
α	Deviator angle between tape segments
β	Elastic foundation characteristic parameter
γ	Degree of tape bending
Δ	Tape bending displacement
δ	Tape groove bearing deformation
ϵ_u	Ultimate Tape strain
θ	Angle defined by the access-slot sector
λ	Shell characteristic parameter
σ_z	Axial (longitudinal) stress
ν	Poisson's ratio
ϕ	Angle of the tape wedge

Tape Joint Design Guidelines

Introduction

Connections are usually the weak point in any structure. Consequently, examination of the behavior and strength of a connection from either an experimental or analytical viewpoint is often required. Standard joint configurations incorporating bolt or screw fasteners are very difficult and/or time consuming to analyze in-depth, and one must usually resort to expensive testing. The accumulated experience of the engineering profession in standard applications often diminishes the need for analysis of common joints. However, the reliability of modified connections or even standard connections in new applications is tenuous. The fact that most structural failures occur at connections underscores this point.

Connections joining cylindrical cases are required in normal applications (such as pipelines) and high performance areas (such as rocket bodies). Easy fabrication and assembly, strength, lightness, and/or space efficiency are necessary in both applications at one time or another. The tape joint concept developed at Sandia National Laboratories can provide these properties. It is stiff and strong in both bending and axial loading; easy to design, analyze, fabricate, and assemble; and space-efficient and lightweight. The tape joint supersedes in versatility most other joints.

Several features of the tape joint had been used individually throughout the years, but they were first combined as a system in the late 1960s (Alvis, 1971). The concept underwent several changes during a development and optimization program during the 1970s (Huerta and Black, 1976).*

There have been a few commercial applications. In the last 5 yr, pipe manufacturers have begun using the concept for fittings. One manufacturer has used the tape joint to join plates to form a box.

This report provides guidelines for designing a cylindrical, interlocking tape joint. Projects in the intervening years have provided experience in the application of the tape joint such that a recommended design procedure can be put forth. Background information, discussion of component features, and methods of numerical analysis are presented to aid the designer in making reasonable modifications to the joint. Examples of modified joints are presented that demonstrate the adaptability and versatility of the joint in unusual situations.

Tape Joint Components

This section introduces the reader to the tape joint concept. It also serves to point out the vital features and their purpose so the designer can make various workable modifications to the standard tape-joint configuration.

Figure 1 shows the general connection features prior to assembly. The joint consists of an inner and outer shell, each with an interlocking tab and tape groove. The interlocking tabs help align the joint and prevent excessive radial deformation when the joint is loaded axially. They also make it capable of withstanding large bending and cross-shear loads. Excessive radial deformation would permit the shells to slide over the tape inserted into the tape groove and cause failure. Thickening the joint or extending the shell well beyond the tape groove also prevents excessive radial deformation. The latter modification was used in an application dicussed in a later section. The significant features (the interlocking tab and tape groove) can be turned on one machine without the need for special tools or setups. In high-performance applications, sharp corners are eliminated to reduce stress concentrations.

Figure 2 shows the assembled joint. The resulting assembly has an internal upset (smooth exterior surface) but it can easily be fabricated with an external upset, as preferred in pipe. The tape grooves in the shells form a tape tunnel. A slight offset of the grooves allows the tape segments to wedge the joint tightly

*References at the end of the report are cited by author and date.

closed. The parts are dimensioned such that there is only one point of closure. This greatly reduces expenses caused by close tolerancing. If the metal-to-metal contact is not sufficient for sealing purposes, standard O-ring seals can be placed at the interlocking tabs (Figure 2). The seal should be located at the interlocking tab that lies between the confined fluid and the tape groove.

Figure 3.a schematically depicts a pair of tapes. The tape segments are machined with a straight taper. A pair of tapes are inserted from opposite directions in the tunnel and produce a variable dimension (w) as illustrated. Increasing the w dimension by moving the tape segments together results in a wedging action in the tunnel and tightly closes the joint. The variable dimension (w) avoids the requirement for close tolerancing of the tunnel in the axial direction. The tapes are purposely fabricated long to accommodate any deficient or excess axial dimension in the tape tunnel.

The designer may use only one tape and omit the wedging action in applications where the joint is loaded exclusively from one direction. A pressure-vessel joint with this modification is discussed in a following section. Some pipe manufactures have adopted this modification for fitting applications.

Figure 3.a also illustrates the slits cut at regular intervals in the tape. The slits facilitate bending of the tapes by forming plastic hinges (Figure 3.b). Thus, the tapes readily adopt a circular shape and ease tape insertion. The tape does not assume a smooth curve but rather a curve formed by a series of straight segments. The slits are spaced such that a straight segment is not forced to bend in the tunnel. Consequently, the slit spacing controls the radial dimension of the tunnel (H). The slit spacing is halved near the tape ends. The increased number of slits facilitates snipping off any excess tape during assembly.

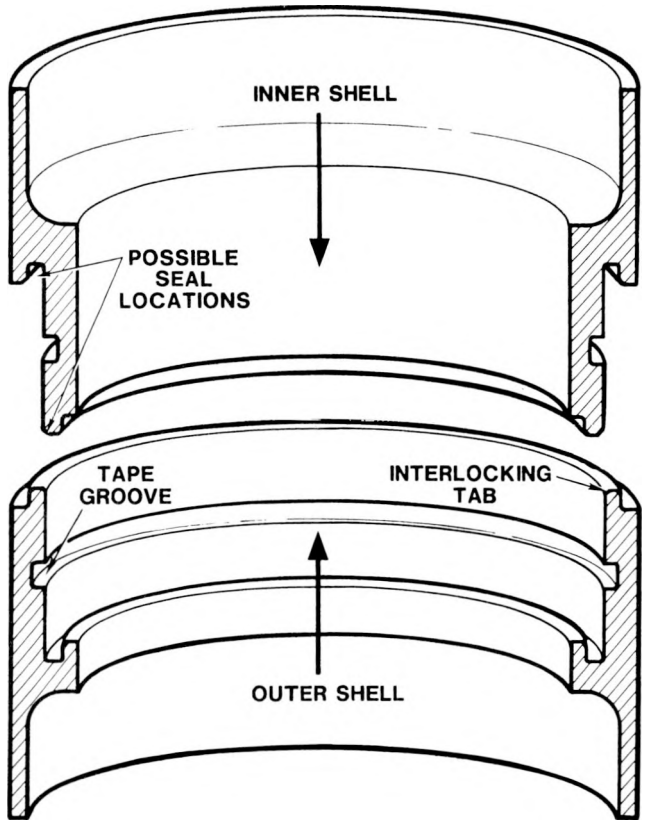

Figure 1. Tape Joint Configuration

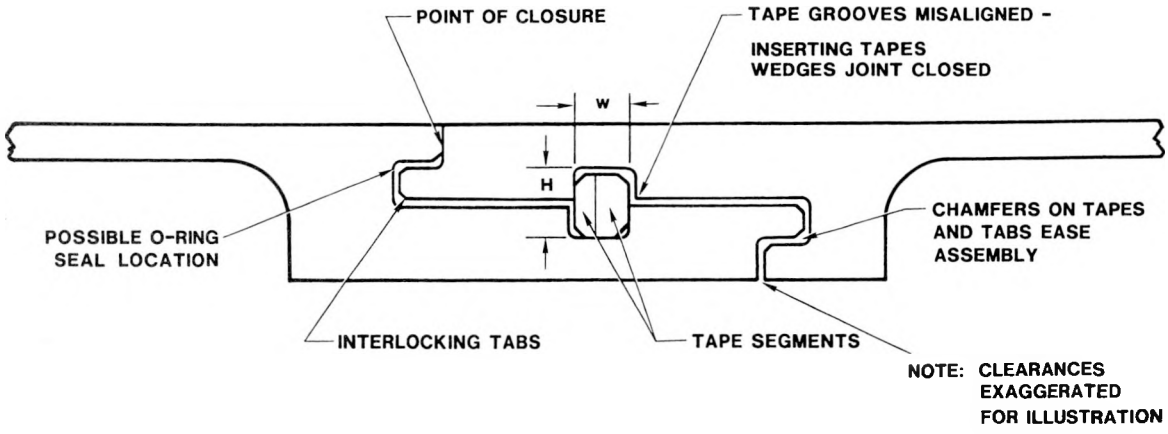

Figure 2. Components of the Tape Joint

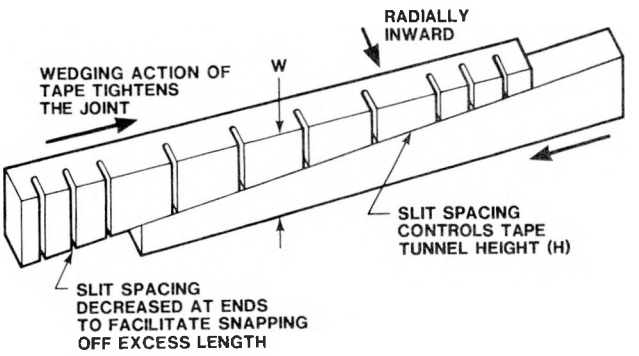

a. Wedging Action

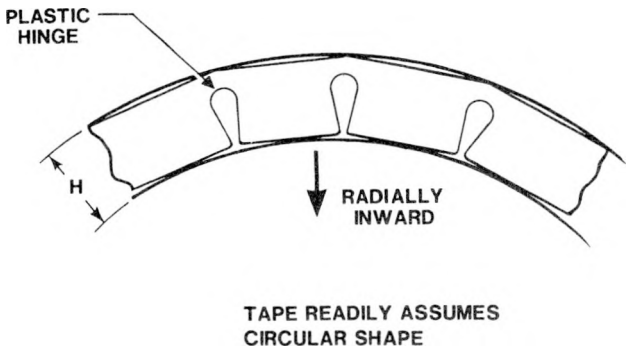

b. Plastic Hinge

Figure 3. Tape Features

Several additional features prevent assembly difficulties. First, the tape tip and edges are chamfered to prevent jamming and to ease insertion of the tape. In high-performance applications, the tapes can be rounded at the edges to fit snugly into the small rounded corners of the tunnel which are formed to avoid stress concentrations. Second, using hardened material for the tapes prevents excessive mushrooming of the tape ends when they are impacted into place.

The tapes are inserted into the tape tunnel through two access slots that are usually cut 180° apart. In the past, access to the tape tunnel has been from the structure's exterior; if slightly larger access slots are cut, access can be from the interior.

The access slots can weaken the joint. In the development tests where failure of the joint was dictated, failure began at the access slot. The induced weakness is easily compensated for by thickening the joint. The necessary increased diameter derives from development work and is more fully explained in the next section. The increased radial dimension at the connection is similar to that needed for a screw joint, but it is about half of that required for bolts.

The increased radial dimension can be minimized by reducing the slot-opening size. The current sizing technique basically assumes the tape must be straight and tangent to the tape tunnel for easy assembly. The next section gives details on this sizing strategy. For situations where maximum efficiency is required, one can construct a special tool or tube that guides the tape through a very small access slot in the tape tunnel. Size reductions of the access slot significantly decrease the stress concentrations around the access slot. In turn, this decreases the additional radial thickness needed to produce a joint strength advantage over the shell.

Depending on the application, it might be desirable to cap the access hole to create a smooth exterior or to diminish corrosion of the tapes if materials susceptible to corrosion are used. In vibration applications, the cap prevents excessive loosening of the tapes.

Figure 4 illustrates the assembly procedure. First, the inner and outer shells are mated. Then a lubricated tape is inserted into the tunnel through either of the two access slots cut 180° apart. (Lubricants compatible with the materials should be used when life of the part is critical.) One tape segment fills 180° of the tunnel. Another tape is inserted through the other access slot in the opposite direction. They are wedged into place by impacting the tape ends. (Impacting the other end of the tape segment in the opposite direction loosens the joint and permits easy disassembly.) A punch or drift pin is useful for the last few hammer blows on the tape during assembly (and disassembly). Excess tape material is then snapped off. Once the first set is in place, a second set of tapes is inserted in the other half of the tunnel.

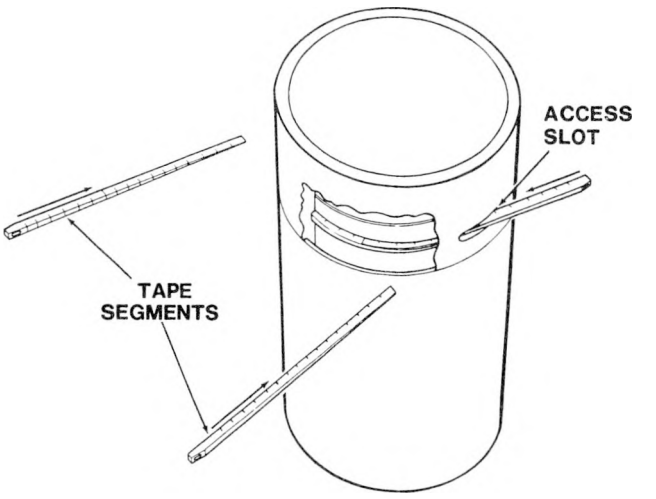

Figure 4. Tape Insertion

As noted in Figure 3, the tape slits are inserted radially inward. This method prevents the sharp slit edges from gouging into the tunnel sides and causing undue assembly difficulties, and prevents an unnecessary decrease in shear area by opening up the slits. The designer must specify sufficient slit width (a) to form the required tape curvature, but normal fabrication techniques typically produce slit widths (a) greatly in excess of this minimum.

Unlike bolted connections, the point of sufficient joint tightness is easily discerned by the individual hammering the tapes into place. A study in which the joint was assembled with a calibrated air hammer was conducted in order to specify uniform tightness (Blose, 1976). However, it has been found that an experienced person can consistently match the assembly joint tightness based on their sense of hearing. As the tapes tighten, the pitch of the hammer impacts rises quickly. One can hear a constant high pitch when the joint is sufficiently tight.

Most difficulties in assembly are eliminated by cutting a long tape and permitting a wide variation in the axial tunnel dimension (w). However, other dimensioning errors can occur. A frustrating situation occurs when the radial dimension (H) is too small; dimensioning such that H is always too large remedies the situation (there is little strength decrease from over-dimensioning). The tape wedging action still clamps the joint shut. An immediate solution, however, is to "get a bigger hammer". The joint pieces and hardened tapes can usually withstand the greater force needed to wedge the tapes into the tunnel, and dissassembly is rarely impeded.

Optimum Tape Joint Dimensions

The complicated shape of most connections prevents accurate analysis. The simple tape joint architecture, on the other hand, permits accurate analysis and subsequent design optimization. The optimum joint dimensions for ℓ, h, w, T, r, and L, defined in Figure 5, is derived from post facto examination of the development work data (Huerta and Black, 1976) and several applications since that time (a few are discussed in the example application section).

The tape joint was optimized, using the performance criterion of mininum radial thickness. Secondary criteria were to maintain a reasonable axial upset length to diminish joint weight, the ease of assembly and fabrication, and cost considerations. An important constraint was the requirement of a joint strength advantage over the structural material (shell).

Figure 5 shows the usual connection where material of similar thickness (t) and type are joined. Note that ℓ, h, and r are equal in both parts, but that T and L differ. These anomalies result from different load paths in the inner and outer joint connection and the location of the tape access slot. A design example presented later discusses a joint connecting cylinders of different thicknesses (t) and material. For this situation, all six dimensions differ in an optimized tape joint.

Optimum dimensions for the inner and outer coupling are discussed first, followed by preferred tape dimensions. However, several tape dimensions affect the part dimensions and are introduced as needed. Specified clearances (tolerances) for proper assembly are an important practical aspect of dimensioning, but discussion of this added complication is deferred until the design section.

Characteristic Shell Length

The length (ℓ) fore or aft of the tape tunnel is an important dimension. It equals the reciprocal of the characteristic λ for a hollow cylinder. The characteristic λ is similar to the concept of the characteristic β for elastic foundations (Hetenyi, 1946):

$$\ell = \frac{1}{\lambda} = \left[\frac{(R_5 t)^2}{3(1-\nu^2)}\right]^{1/4}. \qquad (1)$$

(The nomenclature is listed in the front of the report and in Figures 5 and 10.)

For most design situations, assuming ν equals 0.30 is adequate. Thus, Eq (1) reduces to:

$$\ell_1 = 0.778\,(R_5 t_1)^{1/2}. \qquad (2)$$

To avoid excess radial displacements and bending stresses above or below the tape tunnel and still maintain small radial thicknesses, there must be sufficient length fore and aft of the tunnel. The use of one characteristic length (ℓ) fore and aft of the tunnel is derived from computer modeling. A comparison of stress above or below the tunnel versus the length in front or behind the tunnel plots as a decay curve with a definite knee occurring near a length equal to ℓ. Beyond the knee, the curve plateaus; little decrease in stress occurs with increasing length; hence, ℓ was chosen as an optimum length.

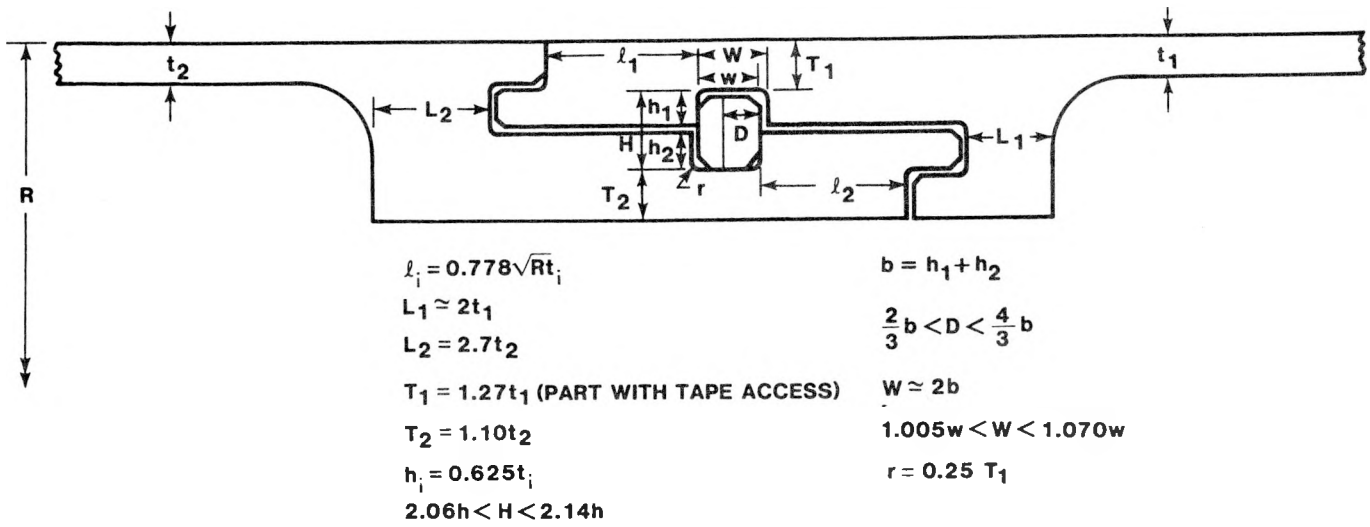

Figure 5. Optimum Tape Joint Dimensions

Dimensions Controlled by Tensile Failures

As with bolted connections, the tape joint could conceivably fail because of excessive

- Tensile stresses in the net section defined by T_1 and T_2,
- Shear stresses in the fastener (tapes) and along the L dimension (tape joint throat regions), or
- Tape bearing loads on the tape groove.

Tensile stress above and below the tape tunnel determines the thickness dimension (T) and is discussed first. Shear stresses in the tape determine the required tunnel-width dimension (w). The tape groove height dimension (h) is determined from the bearing stresses. Subsequent sections discuss these latter dimensions. The optimum values selected are based on the suggested design practice of dictating failure of the structural material (shell) rather than the joint itself. Only in unusual circumstances would this practice be ignored. (The ability to perform accurate analysis on the connection behavior in these unusual situations is a distinct advantage of the tape joint.)

Corner Radius (r). Large tensile stress in the net section above and below the tape tunnel can cause joint failure, but before dealing directly with this failure mode, the subtle effects of the tape groove on the stress concentration in the net section must be discussed. The tape groove creates a notch in the shell material. For ductile material experiencing a steady or steadily increasing uniaxial stress, the corner radius (r) has little influence on the joint behavior; any practical corner radius can be specified. However, the corner radius (r) has a significant influence on the joint member's strength for shock and cyclic loading (fatigue) conditions. It is necessary to specify a corner radius in the groove to avoid sharp-notch problems.

In the experimental parameter optimization program using ductile 6061-T6 aluminum, it was found that an r/T ratio (shell parameter) equal to 0.25 resulted in the desired joint-strength advantage over the shell. For optimum tape joint designs using tough material, the r/T ratio should remain at this value. Thus, once the net tensile section thickness is known, an appropriate corner radius can be selected:

$$r = 0.25\ T_1 . \qquad (3)$$

In order to allow more design latitude, it is desirable to express the test results in terms of a stress concentration factor (K_t). The equivalent K_t is 1.43 if bending moments are neglected and the groove region is assumed to behave as 1/2 of a stepped, flat tension bar with shoulder fillets (Peterson, 1974). Figure 6 presents appropriate r/T curves as a function of K_t and the ratio of the upset thickness (m) to net tensile thickness (T). Figure 6 is based on Peterson's work (1974). Satisfactory joint behavior should result if K_t remains below 1.43 for shock-loading conditions.

From the maximum stress concentration factor of 1.43, known material properties, and an appropriately assumed axial stress for the application under consideration, the fatigue life of the joint may be estimated (Rolfe and Barsom, 1977). For vibration-loading conditions where the axial stress values are low, the joint might easily survive more than 10^4 cycles (Hickerson, 1975).

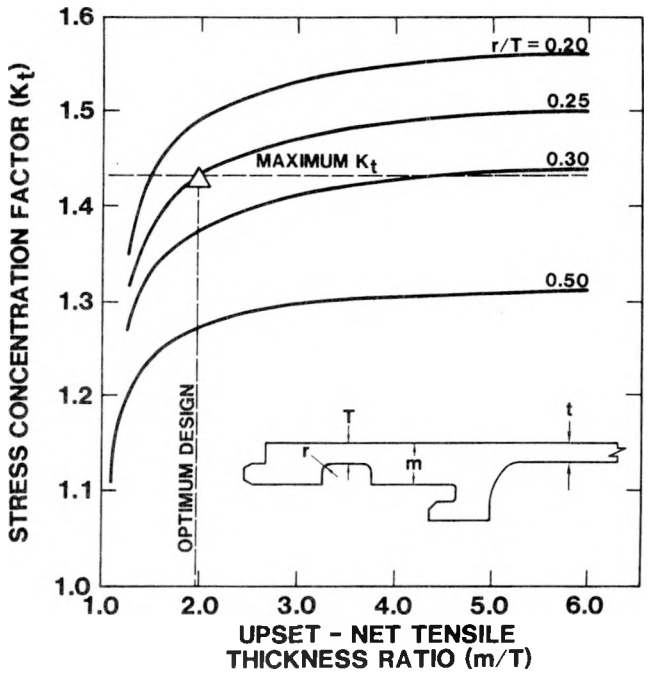

Figure 6. Stress Concentration Factor (K_t) as a Function of the Shell Parameters, r/T and m/T

Net Tensile Section Thickness (T). Tensile stresses above or below the tape groove determine the required thickness (T). Experimental testing on a tough material found that, for the joint coupling without a tape access slot, a T dimension 5% greater than the structural shell thickness (t) induced failure in the shell. To give the joint adequate strength advantage, the thickness should be increased another 5%; thus,

$$T_2 = (1.05)(1.05)t_2 = 1.10\ t_2 \text{ (w/o slot)}. \quad (4)$$

The coupling (either inner or outer) with the tape access slot requires greater thickness to compensate for the lost area and resultant stress concentration. The lost area usually amounts to about 10% if the traditional sizing scheme is used. This is an adequate value for the initial design. Schemes to reduce the slot size would reduce this factor.

Experiments indicate that to compensate for the stress concentration, T must be increased 10% above t. Again specifying a 5% increase to ensure failure in the shell results in an increase above t of 16%. This value coupled with the 10% loss of area caused by the slot itself results in a total increase of 27% necessary to provide the joint adequate strength advantage:

$$T_1 = (1.05)(1.10)(1.10)\ t_1 = 1.27\ t_1 \text{ (w/slot)}. \quad (5)$$

Dimensions Controlled by Shear Failure

Tape Pair Width (w). The term "tape pair width" (Figure 5) defines the width available for the two tape segments wedged into the tunnel. The w dimension is slightly smaller than the tape groove width because of the intentional misalignment.

The second failure mode (shear failure through the tapes) places a minimum value on w. Requiring that failure of the shell occurs before joint failure and assuming that the tape material shear strength is as great as the strongest connector material in the joint and equal to 0.6 of the ultimate tensile strength (F_{tu}) means that w must be greater than 1.67 t. (The thickness (t) corresponds to the strongest connector material in the joint.)

The above minimum is quite small and causes the tape width-to-height ratio (w/b) to be small also. Assembly is much easier if w/b is greater than 2 at the tape tip; this recommended ratio diminishes rolling and twisting of the tapes during insertion. The added axial length of the joint rarely penalizes the design and makes fabrication and assembly easier. More importantly, the added width diminishes tape rolling when the joint is loaded (Figure 7) and thus maintains a larger tape-bearing surface area. Consequently, use of a smaller groove height (h) dimension is possible, as discussed in a subseqent section; hence,

$$w = 2b > 1.67\ t. \quad (6)$$

When materials with the same thickneses are joined, Eq (6) reduces to:

$$w = 4h. \quad (7)$$

Tape Tunnel Width (W). Once the total tape pair width (w) is known, one can determine the tape tunnel width (W) of the joint parts. Figure 5 presents a typical range for W. The percentage increase over w can vary between 0.5% to 7.0%. W − w is equivalent to the necessary offset of the tape grooves in the inner and outer shell parts:

$$1.005\ w \leq W \leq 1.070\ w. \quad (8)$$

Throat Length (L). L is the length between the start of the built-up thickness for the joint and the interlocking tab. Because of the tape joint shape, shear stress failure along the inner shell L_2 dimension can occur. (The load in the outer shell does not pass through this throat region.) Hence, L_2 must be greater

than 1.67t assuming that a material shear strength 40% less than the tensile strength is required.

In addition to the shear stress, the inner shell must support a moment along the L_2 dimension. The moment develops from the eccentricity of the bearing surface on the tape and the axial load along the shell. The test series and subsequent joint analysis showed that sizing L_2 greater than 2.70t eliminated excessive shear and bending stresses in the throat region:

$$L_2 = 2.70t \ . \tag{9}$$

The above value is not optimum. Axial dimensions are not usually as critical, so there has not been development testing or detailed optimization analysis conducted on this dimension.

When joining different shell thicknesses, the critical L dimension is not necessarily axial in direction. The example of a tape joint design joining different materials as given in the example section depicts this situation.

The outer shell throat region (region along dimension L) is not critical. This region is not loaded except when large bending deformations cause the interlocking tab to apply a moment. Thus, dimension L must be as large as the interlocking tab dimension. This value is sometimes small, so fabrication considerations or the desire for a symmetrical appearance might dictate a larger value. Two times t is often used:

$$L_1 = 2t. \tag{10}$$

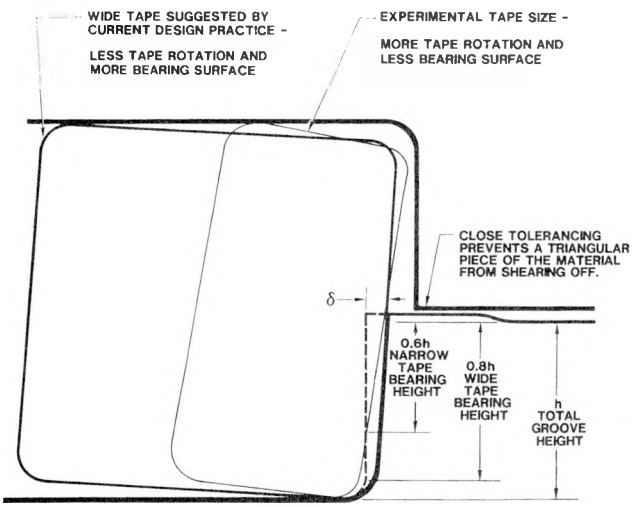

Figure 7. Tape Rolling in Narrow and Wide Tapes

Dimensions Controlled by Bearing Failure

The fastener or tape begins to plow through the structural material and causes large deformation in the bearing failure mode. Figure 8.a shows the bearing-failure mode for a bolted connection (Fisher and Struik, 1974). Figure 8.b shows the bearing-failure mode in a tape joint. The tape joint failure mode was surmised from microscopic inspection of the tape region of a specimen taken to near failure (Figure 9).

Besides the tape-bearing failure on the tape groove face, shear failure is possible (Figure 8.c). Conceivably, a small triangular piece of material could shear off behind the tape if the tolerance gap became too great. The shear failure occurs at ~0.6 of the bearing-failure strength. Hence, designing for the shear failure mode would result in much larger tape groove heights (h). Consequently, the shear failure mode is eliminated by requiring tight tolerances on the joint interface surfaces (radial dimension R in Figure 10) for at least a distance equal to h.

Tape Groove Height (h). Structural material failure as opposed to bearing-load failure is ensured by sizing h such that the height of the material subjected to the bearing load times the bearing capacity of the material (F_{bru}) is greater than the cylinder shell thickness (t) times the ultimate cylinder tensile strength (F_{tu}).

It is important to maximize the contact height between the tape and the groove in order to minimize h. The enlarged photograph (Figure 9) shows that the material carrying the bearing load is ~0.6 of h for the tape proportions used in the experimental tests (Figure 7). As also shown in Figure 7, the bearing contact surface area is increased if the tape w/b ratio is increased. The rotation for the wide tape was constructed using the same groove height (h) and the same material deformation (δ). The resulting contact height is almost the full height (h) of the groove. The corner contact is not fully effective because of the corner radius; thus, an effective height of (h − r/2) is suggested. (Recall that a ratio for r/T of 0.25 was recommended previously.) Expressing the above statements mathematically and solving for h yields:

$$(h - r/2)\, F_{bru} \geq t\, F_{tu}$$

$$h \geq r/2 + (F_{tu}/F_{bru})t. \tag{11}$$

For preliminary design calculations, it is usually sufficient to assume the ratio of F_{tu} to F_{bru} is 1/2 and that the corner radius (r) is 0.25 of the shell material thickness (t). Therefore, the height for h is approximately

$$h_1 = 0.625t_1. \tag{12}$$

Equation (12) will provide a reasonable estimate for the h dimension in most cases.

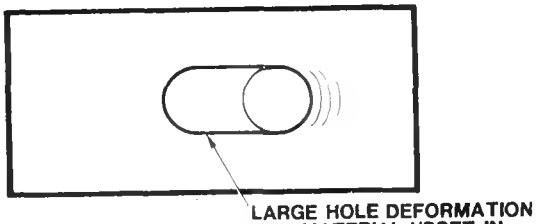

a. (after Fisher and Struik, 1974)

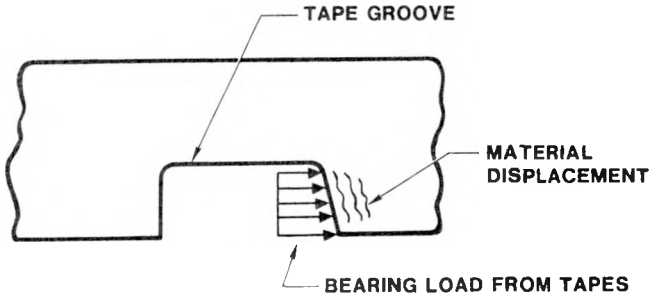

b.

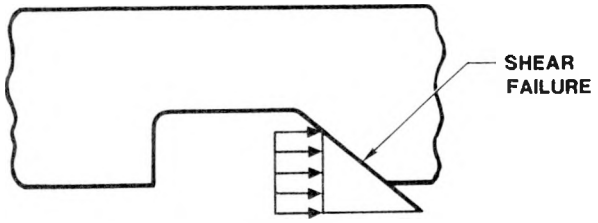

Figure 8. Bearing Failure Modes of Tape and Bolted Joints

Tape Tunnel Height (H). H equals the sum of the two tape groove heights ($b = h_1 + h_2$) plus an additional 3% to 7% of h to account for space (h_s) necessary to accommodate a straight tape segment (Figure 10). Experience in applying the tape joint determined this appropriate range for h_s; therefore,

$$2.06\ h < H < 2.14\ h. \tag{13}$$

When tolerancing is crucial or different material is joined, a more precise calculation can be made for the radial dimension (H) which incorporates an exact value for h_s. The calculation requires the tape slit spacing (p) and the net tensile section thickness (T). The tape slit spacing (p) dimension has not been discussed, but we will assume it is known.

The calculations proceed as follows. Assuming R_5 and T_1 are known, one determines R_4 simply by substracting T_1 from R_1. (For the joint with a smooth interior surface, one would add the radial dimension T_1 to R_1 and progress radially outward with the calculations rather than inward.) Thus,

$$R_4 = R_5 - T_1. \tag{14}$$

The h_s dimension is determined by observing:

$$\sin\frac{\alpha}{2} = \frac{p/2}{R_4} \tag{15}$$

and

$$\cos\frac{\alpha}{2} = \frac{R_4 - h_s}{R_4}\ . \tag{16}$$

Solving for h_s from Eqs (15) and (16) yields:

$$h_s = R_4\left[1 - \cos\left(\sin^{-1}\frac{p/2}{R_4}\right)\right] \backsimeq p^2/(8\,R_4)\ . \tag{17}$$

The corresponding formula for a joint with an external upset (smooth interior) is:

$$h_s = \left[(p/2)/\sin\left(\tan^{-1}\frac{p/2}{R_3 + h_2}\right)\right] - (R_3 + h_1) \backsimeq p^2/[8\,(R_3 + h_1)]\ . \tag{18}$$

(The above approximations are valid as long as the terms $[p/(2R_4)]^2$ or $\{p/[2(R_3 + h_1)]\}^2$ remain less than 0.10, which is usually the case.) The tunnel height is the sum of h_1, h_2, and h_s:

$$H = h_1 + h_2 + h_s. \tag{19}$$

The other radial dimensions are readily found as follows. First, the relationship for R_3 shown in Figure 10 is:

$$\cos\frac{\alpha}{2} = \frac{R_3 + h_1}{R_4}\ .$$

Evaluating R, using Eq (17) yields:

$$R_3 = R_4 - (h_s + h_1). \quad (20)$$

The values for R_2 and R_1 clearly are:

$$R_2 = R_3 - h_2 \quad (21)$$

and

$$R_1 = R_2 - T_2. \quad (22)$$

Access Slot Length (s). The access slot length (s) is not controlled by either the bearing, shear, or tensile failure modes; however, it does have a profound effect on the tensile strength of the joint. In the tape joint development tests, failure began at the access slot in all cases (Huerta and Black, 1976). This topic could be discussed under dimensions controlled by the tension failure mode, but the access slot length is influenced by the tape tunnel height (H) determined above. Also, the calculations parallel those just presented.

Because the tapes must be driven in or out, easy assembly requires that the tapes enter straight and tangent to the tape tunnel (Figure 10). In normal situations, tapes enter the slot from both directions and thus the access slot must remove a portion (~10%) of the outer (or inner) shell. In one application, only a single large tape was used; therefore, only a small aperature was needed for the tape rather than two large slots.

The following sizing scheme applies to external access holes. An internal access slot requires about a 3% increase in size. Figure 10 shows the simple calculation necessary to size s. The formula is readily derived by observing that:

$$s = R_5\theta$$

and

$$\sin\frac{\theta}{2} = \frac{H + T_1}{y}.$$

(The arc length of the slot (s) is not shown in Figure 10.) For small values of θ, $y \backsimeq s$ and $\sin\theta/2 \backsimeq \theta/2$; thus,

$$y = [2R_5 (H + T_1)]^{1/2}. \quad (23)$$

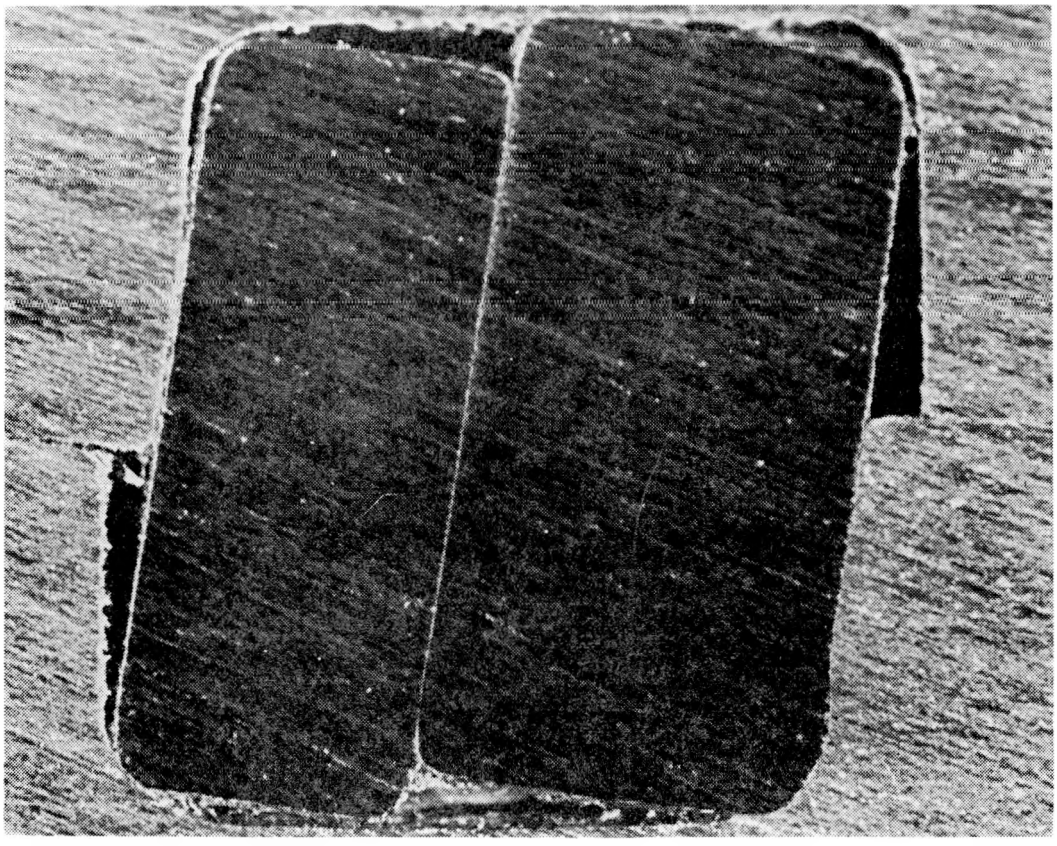

Figure 9. Rolling and Relative Slip of Tape Sections Experienced in 6061-T6 Aluminum Tape Joint Test Specimen With 4340 Steel Tapes Near Maximum Static Load

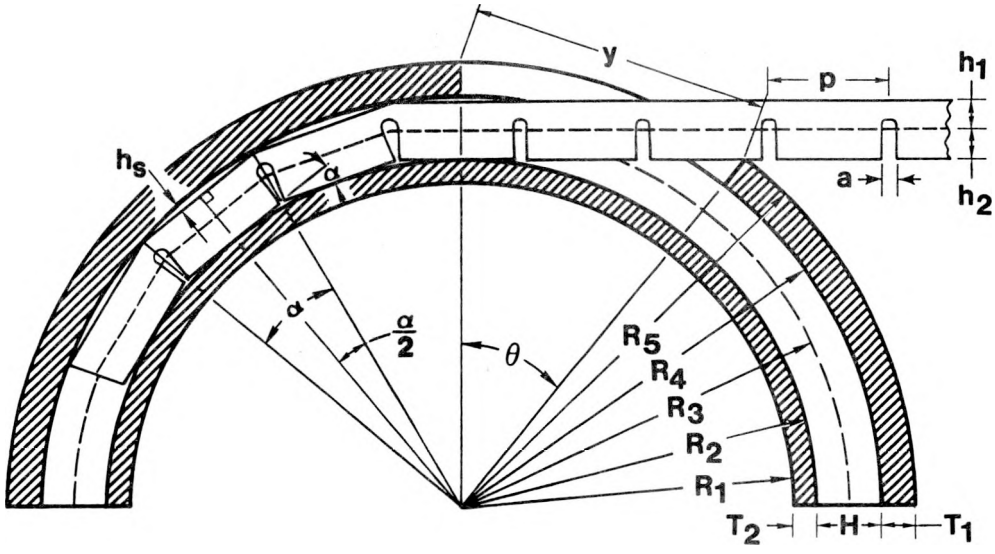

$$h_s = R_4\left[1 - \cos\left(\sin^{-1}\frac{p/2}{R_4}\right)\right] \qquad R_4 = R_5 - T_1$$

$$H = h_1 + h_2 + h_s \qquad R_3 = R_4 - (h_s + h_1)$$

$$y = [2R_5(H + T_1)]^{1/2} \qquad R_2 = R_3 - h_2$$

$$R_1 = R_2 - T_2$$

Figure 10. Calculation of Access Slot Length and Tape Tunnel Height

The total radial dimension increase necessary for a joint with a sufficient strength advantage to ensure failure in the structural material is 3.63t for tough materials (tolerance gaps have been neglected):

$$R_5 - R_1 = 3.63t.$$

Oil well casing threaded joints are weaker than the casing itself, but it is instructive that, for buttress or round thread joints, the upset radial thickness is about 2.63t (API, 1976).

Tape Dimensions

The tape dimensions (height (h) and total tape width (w)) were introduced earlier. The tape height (b) equals the sum of h_1 and h_2, and w is found by using Eq (6) or (7). The necessary tape length (x) when two access slots are specified is πR_4 plus 10%. The additional tape length allows a greater range in the tape width (w) and eliminates the need for close tolerancing:

$$x = 1.10\,\pi R_4. \tag{24}$$

The tapes used in the joint have two additional distinctive features. They are tapered to develop a wedging action and they are slitted to facilitate bending. The slits would not be necessary in very small tapes and/or made from highly ductile material.

Tape Taper. The required taper is easily calculated from the requirement of a minimum w/b ratio of 2, the tape pair width (w), and the necessary tape length. The slope or angle of the wedge (ϕ) is (Figure 11.a):

$$\tan\phi = \frac{2b/3}{x}. \tag{25}$$

An individual tape width dimension (D) (Figure 5) varies between (assuming w = 2 b):

$$\frac{2}{3}b \le D \le \frac{4}{3}b. \tag{26}$$

Tape Slit Width (a). As seen in Figures 10 and 11, the slot width (a) must be great enough to allow a deviated angle of α without the slot completely closing. One tape segment is reproduced in Figure 11.b. It is readily shown that the minimum tape slit width is:

$$a = 2b \tan\left(\sin^{-1}\frac{p/2}{R_4}\right) \simeq 8bp\,R_4/(8R_4^2 - p^2)\,. \quad (27)$$

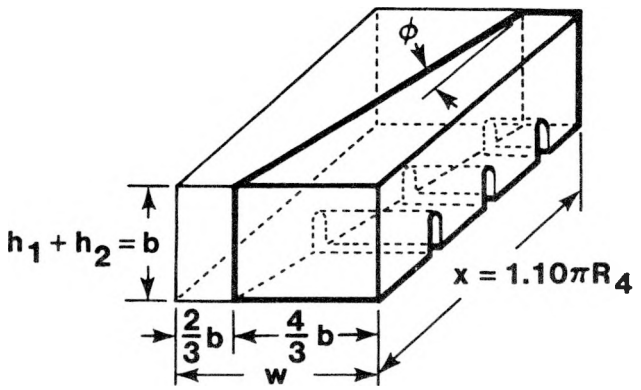

a. Tape

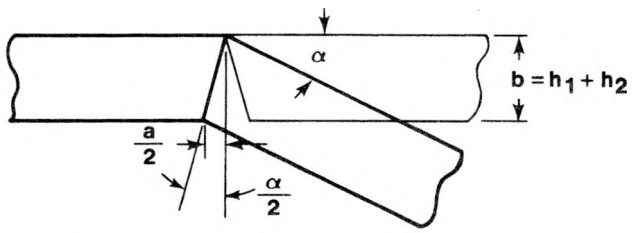

b. Schematic

Figure 11. Tape and Schematic Tape Dimensions

The tape slit is formed by simply cutting into the tape. Convenient saw blade widths larger than the minimum from Eq (27) can be used. Figure 12.a shows the optional use of a drill hole to terminate the slit. This can reduce production costs because control of the slit cutting can be less precise. Also, alternate cutting techniques such as electrical or chemical cutting can be used. In addition, the drill holes produce a better hinge because stresses are more uniformly distributed throughout the plastic hinge area. This, in turn, reduces the possibility of fracture; however, we have never experienced a fracture.

Tape Slit Pitch (spacing) (p). Several calculations make use of the tape slit pitch (p) (Figure 12.a). Its value is arbitrary, but experience has shown values between 0.5 and 0.75 in. (13 to 19 mm) are best when joining cylinders between 1 and 2 ft (0.3 to 0.6 m) in diameter. One application required a single 1-in.(25-mm)-wide tape for joining 40-in.(1-m)-dia cylinders. In this case, 1-in. (25-mm) spacing was used.

Minimum Tape Hinge Depth (d). The ultimate strain (ϵ_u) of the tape material dictates the minimum tape-hinge depth (d). In order to develop an appropriate formula, first assume that a uniform bar of rectangular cross section is bent into a circular arc (Figure 12.b). Let the bar represent the region above the tape slits. The bar height is then d. The maximum strain (ϵ') in the bar is:

$$\epsilon' = (R_0\gamma - x)/x\,.$$

If no strain occurs at the bar midpoint, the original length equals:

$$x = \gamma R_m$$

where

$$R_m = R_0 - d/2\,;$$

hence,

$$\epsilon' = \frac{R_0}{R_0 - d/2} - 1\,. \quad (28)$$

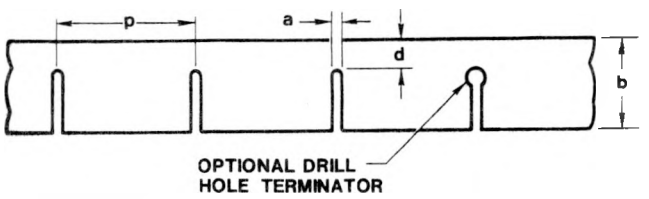

a. Slit Width

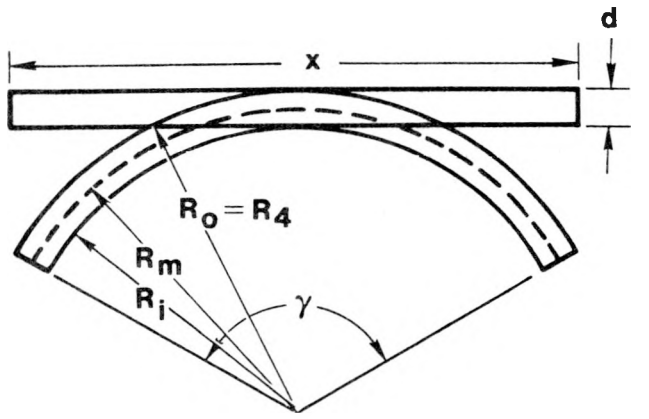

b. Minimum Hinge Depth

Figure 12. Slit Width and Minimum Hinge Tape Dimensions

The bending displacement (Δ) that occurs in the extreme fiber is equal to:

$$\Delta = (np)\,\epsilon'$$

where n refers to the number of segments of length p (Figure 12.a). For our case, assume all of the strain in the tape occurs above the slit and within the distance a. Consequently, the bending displacement (Δ) now occurs within the length na. Let ϵ represent the slit strain; then:

$$\Delta = (na)\,\epsilon.$$

Equating the two expressions for the bending displacement yields:

$$a\epsilon = p\epsilon'.$$

Substituting for ϵ' in Eq (28), solving for d, and noting $R_0 = R_4$ yields:

$$d = \frac{2aR_4\epsilon}{p + a\epsilon}. \qquad (29)$$

The minimum slit depth occurs when the strain equals the ultimate strain (ϵ_u). An alternate equation is found, assuming $R_4 = R_3 + d/2$. This is not strictly correct, but the error introduced is inconsequential:

$$d = 2R_3\epsilon_u a/p.$$

Observe that d increases with increasing slit width (a).

From a structural standpoint, tape fractures in the radial direction caused from overstraining at the slit are not of concern. The joint still performs satisfactorily with radial through-cracks. A minimum hinge depth is specified to ensure satisfactory assembly and disassembly. With radial through-cracks, assembly and disassembly might be possible because the tape is hammered in and out in most cases but it could be difficult.

Design Procedure

Preliminary Data

Preliminary decisions are needed on the following items before proceeding with the design calculations.

- What is the necessary diameter of the case?
- What type of case material is needed for the application? (Selection of the material might depend on the joint dimensions in some situations. Iteration of the design would be required.)
- Does the application require a smooth inner or outer surface?
- How many access holes and tapes? (There are usually two access holes and four tapes.)
- What are the tolerancing requirements? Is this a high performance application?
- Are seals needed?

Data needed for the design calculations are:

- Cylinder outside diameter (or inside diameter if a smooth interior is required)
- Strength characteristics of the cylinder (acceptable approximations for F_{su}, F_{bru}, and ν are shown in parentheses):
  - Shell thickness for each joint connection (t_1 and t_2)
  - Ultimate tensile strength (F_{tu})
  - Ultimate shear strength ($F_{su} = 0.6\ F_{tu}$)
  - Ultimate bearing strength ($F_{bru} = 2\ F_{tu}$)
  - Poisson's ratio ($\nu = 0.30$)

Design Steps

An integral part of the design procedure is the selection of tolerances. Appropriate tolerancing ensures easy assembly of the joint and predictable behavior, but close tolerancing greatly increases fabrication costs. Figures 5 and 13 provide an exaggerated view of the tolerance gaps for a typical joint. Note on Figure 13 that one longitudinal dimension of the tape groove and dimensions R_3 and ℓ require close tolerancing.

Tolerancing is judgmental and not easily formulated, but there are four general guidelines to keep in mind when tolerancing the tape joint:

- Tolerance the axial dimensions to ensure closure at only one point. This permits a larger tolerance range on most dimensions.
- Tolerance the axial position of the tape grooves to ensure a misalignment such that tape insertion wedges the joint closed. This requires a somewhat close tolerance on the location of one end of the tape groove with respect to the point of closure.
- Provide a tight tolerance on the radial dimension R_4. Costs can be reduced on joints with long tunnel separation lengths (ℓ) by only requiring close tolerances near the tunnel and the interlocking tab.
- The dimension values calculated in the following design steps are the minimum accepted values. Tolerance the radial and axial dimensions such that they are never less than these minimums.

From the preliminary data and tolerancing concepts, one can proceed through the 12 design steps given below. As with most designs, certain calculations are interdependent and iteration is conceivable. However, the following steps and the equations selected eliminate iteration in all but very refined designs. The equation numbers listed refer to those in the previous section.

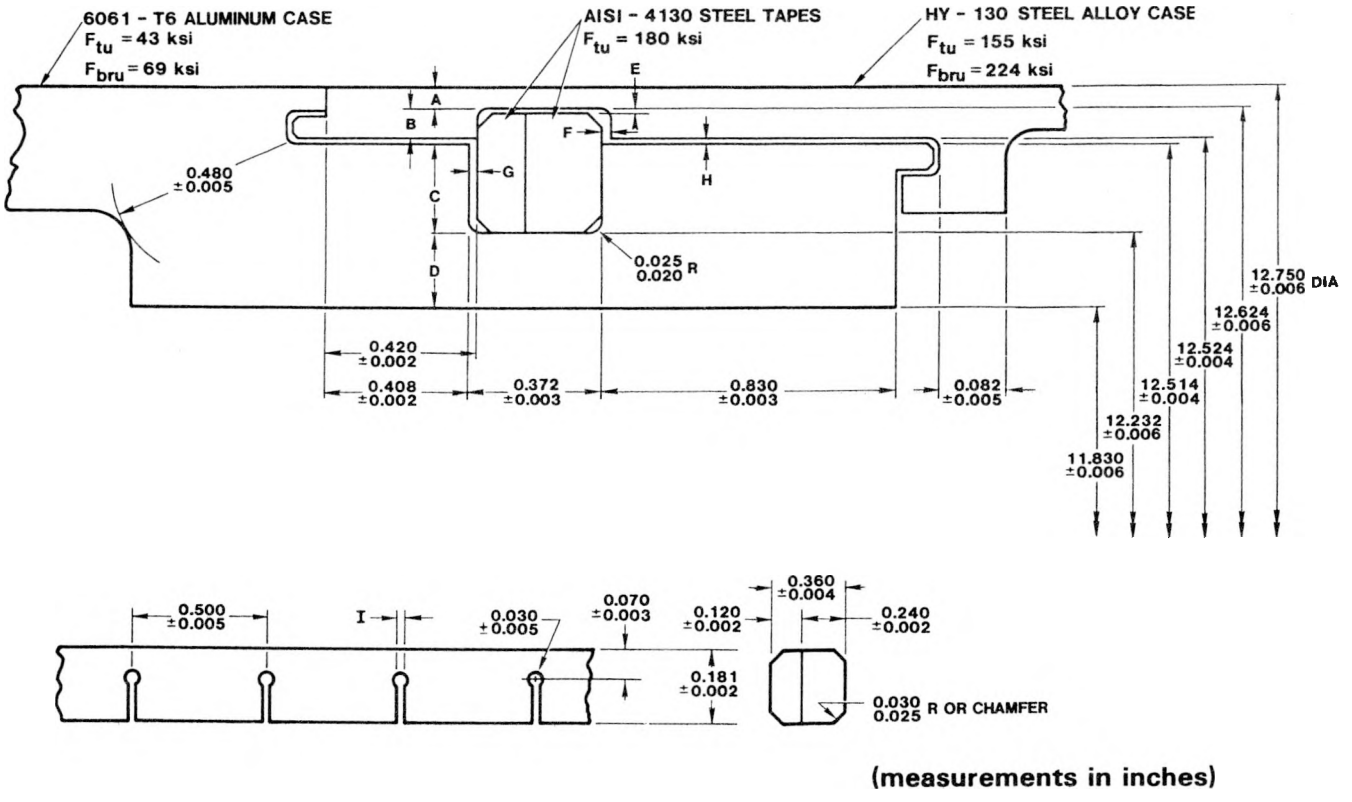

Figure 13. Example of a Tape Joint Design Joining Different Materials

Radial Dimensions

Step 1. Select a slit spacing (p) for the tapes. Below are appropriate values based on experience (Figure 12).

Case Diameter ($2R_5$) (ft/m)	Pitch (p) (in./mm)
1.0/0.3	0.50/13
2.0/0.6	0.75/19
3.0/1.0	1.00/25

Step 2. Calculate the net tensile thickness (T) for each joint connection (Figure 5). For applications using 1 or more than 2 access slots and more refined calculations, use a more accurate estimate of the slot length. This will modify the factor in Eq (5).

$$T_2 = 1.10t_2 \quad \text{(w/o slot)} \tag{4}$$

$$T_1 = 1.27t_1 \quad \text{(w/slot)} \tag{5}$$

Step 3. Calculate the tape groove heights (h) and the groove corner radius for each joint connection (Figure 5). (Use Eq (11) for more precise designs.)

$$h_1 = 0.625\ t_1 \tag{12}$$

$$r = 0.25\ T_1 \tag{3}$$

Step 4. Determine the radial dimensions. Note that the following formulae assume an exterior tape access slot and internal upset joint (Figure 10).

$$R_4 = R_5 - T_1 \tag{14}$$

$$h_s = p^2/(8R_4) \tag{17}$$

$$H = h_1 + h_2 + h_s \tag{19}$$

$$R_3 = R_4 - (h_s + h_1) \quad \text{(close tolerance)} \tag{20}$$

$$R_2 = R_3 - h_2 \tag{21}$$

$$R_1 = R_2 - T_2 \tag{22}$$

Axial Dimensions

Step 5. Determine the tunnel separation length (ℓ) for the inner and outer shells (Figure 5). Use a close tolerance on the tunnel separation length (ℓ) from the point of closure. (Use Eq (1) if dimensioning is critical.)

$$\ell_1 = 0.778\ (R_5 t_1)^{1/2} \tag{2}$$

Step 6. Evaluate the tape height (b), tape pair width (w), and the tape tunnel width (W) (Figure 5).

$$b = h_1 + h_2$$
$$w = 2b \tag{6}$$

$$W = 1.0375\ w \quad \text{(average value)} \tag{8}$$

Step 7. Determine the throat length (L) for the inner and outer shells (Figure 5).

$$L_2 = 2.70t_2 \quad \text{(inner)} \tag{9}$$

$$L_1 = 2t_1 \quad \text{(outer)} \tag{10}$$

Tape Slot and Tape Dimensions

Step 8. Evaluate the tape slot length (y) (Figure 10). After calculating y, return to Eq (5) for refinement of T_1 if a high performance design is required.

$$y = [2R_5\ (H + T_1)]^{1/2} \tag{23}$$

Step 9. Determine the tape length (x) and individual minimum and maximum tape width (D) (Figures 5 and 11).

$$x = 1.10\ \pi R_4 \tag{24}$$

$$\frac{2}{3}b \leq D \leq \frac{4}{3}b \tag{26}$$

Step 10. Calculate the minimum tape slit width (a) and the minimum hinge depth (d) (Figure 12).

$$a = 2b \tan\left(\sin^{-1}\frac{p/2}{R_4}\right) \quad (27)$$

$$d = \frac{2a\,R_4\,\epsilon_u}{p + a\,\epsilon_u} \quad (29)$$

Tolerancing and Miscellaneous Features

Step 11. Dimension the interlocking tabs. The radial thickness equals 1/2 the available radial distance. The tab axial length equals or exceeds the radial dimension (Figure 5). If O-ring seals are required in the tab groove, provide sufficient space to develop the recommended compression. Locate the O-ring seal at the interlocking tab that lies between the confined fluid and the tape groove. Also specify chamfers or radii on sharp corners as depicted in Figure 5.

Step 12. Do a tolerance study. Ensure that there is closure at only one point. Determine the tolerance range in the tape tunnel to ensure easy assembly.

refinement was achieved by substituting the equations incorporating the accurate material properties in the standard design steps. No design iteration was required. The calculated dimensions are easily duplicated by the reader. For example, the groove height in the steel case calculated from Eq (4) is 0.028 in. (0.71 mm). A 0.025-in. (0.64-mm) radius or chamfer on the tape would remove 89% of this height. This percentage is greater than the 20% reduction in bearing surface height caused by the tape rotation (Figure 9). Thus, the groove height (h) must be calculated using Eq (11). The groove height (h_s) equaled about 0.045 in. (1.14 mm) of the thickness (t) by this method.

Several items on Figure 13 deserve comment. First, the calculated tunnel separation length (ℓ = 0.830 in. = 2.11 mm) is a long distance to hold at a ±0.002-in. (0.051-mm) tolerance. Costs could be reduced by relaxing the tolerance between the tunnel and interlocking tab. Second, the minimum throat length (L) for the aluminum case is not in the axial direction; the L dimension applies to the minimum cross-sectional area. Finally, the minimum plastic-hinge depth (d) shown for the tape is based on an assumed slit width of 0.020 in. (0.51 mm). Once the exact method of forming the slit is known, a more accurate value can be specified.

As an aid to the designer, values for the maximum and minimum tolerance gaps are tabulated in Table 1. This tolerance study is part of Step 12 in the design procedure.

Application Examples

Several tape joint examples are shown to illustrate design possibilities.

Tape Joint Example Joining Different Materials

Figure 13 shows a preliminary tape joint design mating a 0.045-in.(1.14-mm)-thick HY-130 steel case with a 0.175-in.(4.44-mm) 6061-T6 aluminum case. (Dimensions in Figure 13 are shown in inches.) Dif ferent shell thicknesses were necessary to provide equivalent strength under axial loads. The other features of the tape joint are quite standard.

This preliminary design was for a high-performance application where the tapes might have to be pulled to disassemble the joint. The necessary design

Conical Section and Pressure-Vessel Tape Joints

Figure 14 shows a full-scale drawing (with exaggerated tolerance gaps) of a tape joint used in a conical section. The tape joint was used in three places in the section; thus, the tape was standardized to reduce costs. Adaption of the design principles was straightforward.

Figure 15.a is a sketch of a large tape joint in a pressure vessel. Quick assembly of the vessel was a stipulated specification of the design. Speedy assembly is possible with a tape joint. Even a large 1 × 3/4 in. (25 × 19 mm) tape can be quickly driven into the tape tunnel. The eight small setscrews used to remove slack could be tightened much faster than numerous bolts. The tape joint also eliminated problems with dirty threads and the need for special equipment to turn and tighten a threaded joint.

Table 1. Tolerance Study of Example Tape Joint Design

Designated Dimension	Calculated (in./mm)	Nominal (in./mm)	Minimum (in./mm)	Maximum (in./mm)
A	0.057/1.45	0.063/1.60	0.057/1.45	0.069/1.75
B	0.045/1.14	0.050/1.27	0.045/1.14	0.055/1.40
C	0.136/3.45	0.141/3.58	0.136/3.45	0.147/3.73
D	0.195/4.95	0.201/5.11	0.195/4.95	0.207/5.26
E	0.005/0.13	0.015/0.38	0.007/0.18	0.023/0.58
F	—	0.012/0.30	0.002/0.05	0.022/0.56
G	—	0.012/0.30	0.008/0.20	0.016/0.41
H	—	0.005/0.13	0.001/0.03	0.009/0.23
I	0.015/0.38	0.020/0.51	0.015/0.38	—

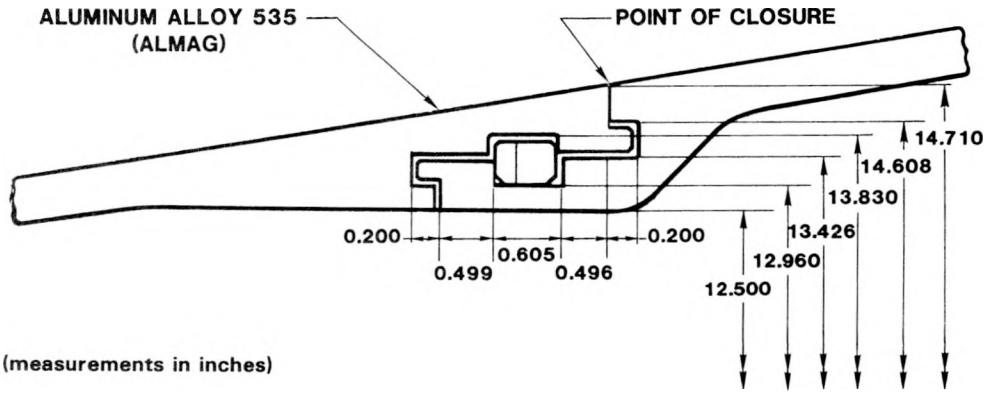

Figure 14. Tape Joint in Conical Section

No tape wedging action was required because the joint loading was exclusively from one direction. Four access slots were used in this design. Only one tape had to enter at each point; thus, a small insertion opening could be used for the four single tapes. Each of the four tapes were formed from 9-in. (0.23-m) segments. The segments were tied together with a single stud screw at the segment end to form the tape (Figure 15.b). This technique greatly reduced the cost of the tape fabrication.

Joint disassembly required that the tape be pulled out. A minimum plastic-hinge depth (d) was calculated (Eq (30)), and the tape slits were terminated with drill holes to prevent unnecessary stress concentration. These steps limited the possibility of breaking the tape.

The O-ring shown in Figure 15.a provided a sufficient seal to maintain 1100-psi (7.6-MPa) pressure in the vessel.

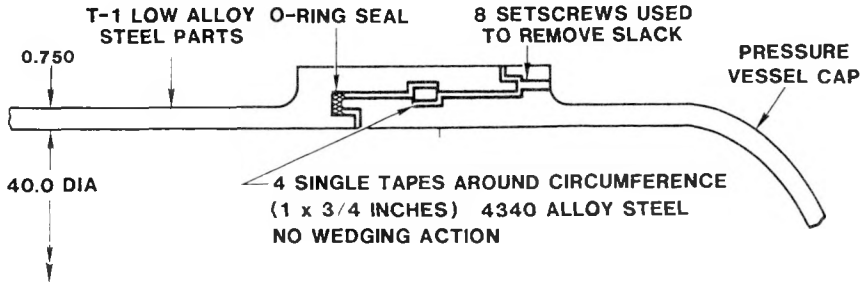

a. Shell

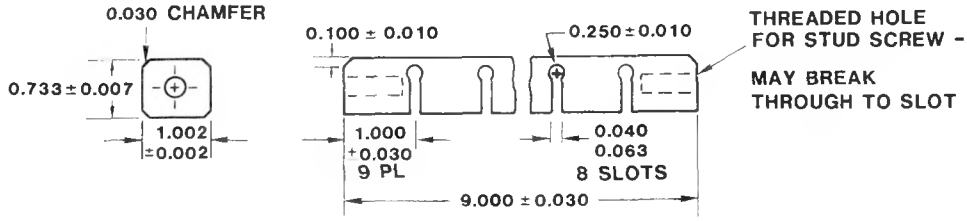

(measurements in inches)

b. Large Economical Tape

Figure 15. Pressure Vessel Tape Joint

Tape Joint Without Interlocking Tabs

Figure 16 shows a highly modified tape joint mating a 6061-T6 aluminum case to a 15-5PH, H1100 stainless-steel case. Insufficient space existed in the radial direction for a structurally adequate, bolted connection; furthermore, the assembly method did not permit turning the inner or outer shell for a threaded joint. Thus, alternate connections were quickly ruled out. However, the tape joint could not be used without modification. The following discusses the procedure used to adapt and analyze the modified joint.

The joint design started with the standard dimensioning scheme for the tape and tunnel. Because of nonstructural shielding surrounding the aluminum case, space was not sufficient for the traditional interlocking tabs used to prevent radial deformation. On this particular joint, internal support greatly diminished radial deformation of the aluminum part. However, the steel shell had to be extended beyond the tape tunnel to limit its radial deformation. Initially, the shell was extended one characteristic length (ℓ). The radial dimension at the end of the extended steel shell was changed slightly halfway down to permit a change in tolerancing.

After the initial sizing, the joint pieces were analyzed individually with the finite-element program SASL to provide insight into the joint behavior. SASL is a static, linearly elastic, 2-D, finite-element program that is fast, inexpensive, and easy to use (Biffle, 1974). The computer models of the individual parts ignored part-interaction contact forces. The peak tension from the dynamic-load history (Figure 17) was applied statically at the point of closure.

Several dimensional modifications were made based on the results. First, the steel shell was lengthened because the predicted edge deformation was larger than desired. Second, the transition from the shell to the joint in the aluminum part was smoothed because of a stress concentration at the throat. The modified transition did not remove the stress concentration entirely (as shown by subsequent computer runs on the modified shape), but the small region above the yield stress did not justify further modifications. In addition to dimensional modifications, the stresses calculated in the steel-casing model indicated the appropriate strength (heat treatment) of the stainless steel to be selected.

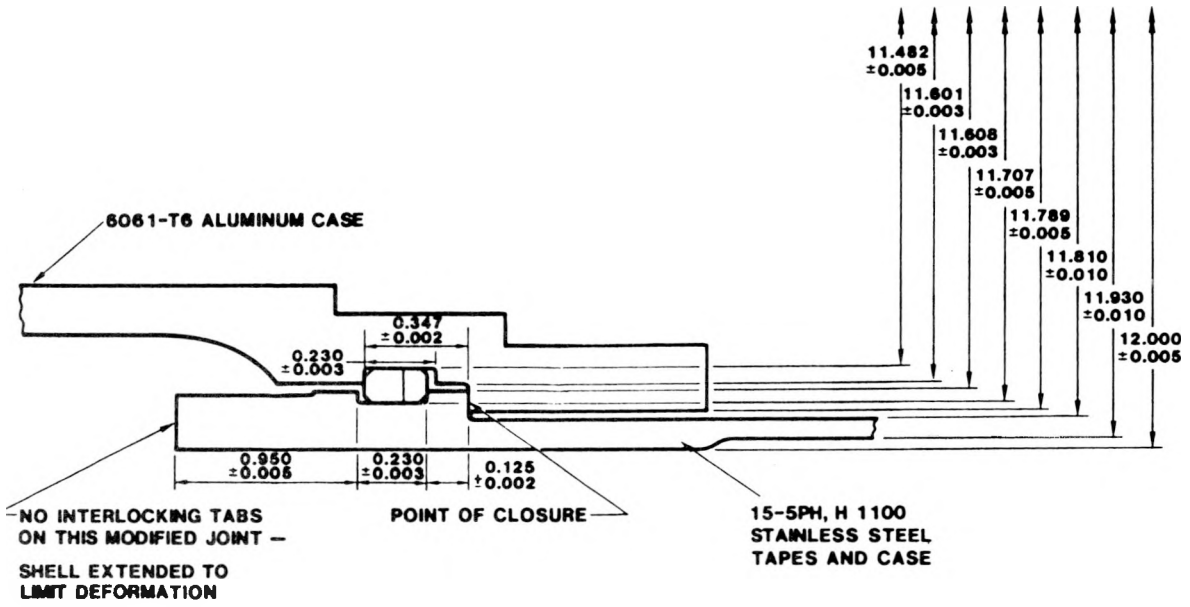

Figure 16. Tape Joint Without Interlocking Tabs

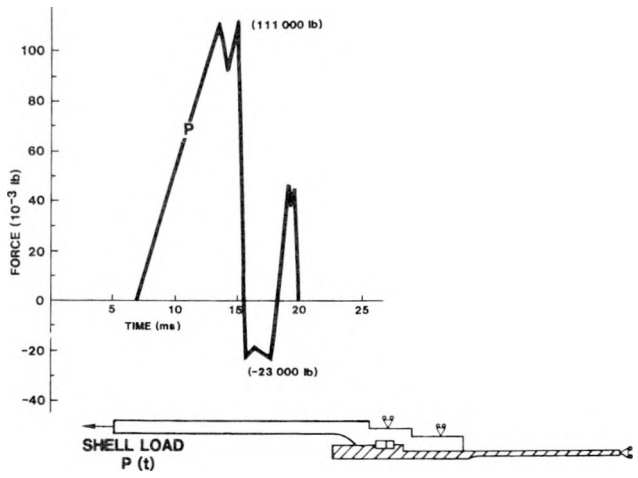

Figure 17. Modified Tape Joint Boundary Conditions

With most designs the analyst would stop here, satisfied that the joint would behave properly. However, the importance of this particular joint and the inability to adequately test the connection experimentally provided an impetus to develop a more detailed model using HONDO II (Key et al, 1978). HONDO is a dynamic (explicit time integration), 2-D, large deformation computer program that can model inelastic, nonlinear material behavior. Slide line capability permits the examination of the interaction of parts in the tape joint.

The boundary conditions and forcing functions applied to the HONDO model are shown in Figure 17. A 7.0-ms delay occurs between application of the loads to the entire structure and the loads significantly affecting the tape joint component. Infinite end boundary conditions were assumed at a distance of 4ℓ from the joint. No frictional forces were assumed in the model; in addition, no assembly preload stresses from the tape wedges or the aluminum nut were assumed. Preload stresses are negligible compared to peak-loading conditions. Finally, sharp corners were used throughout the model (tape groove included) because tough, ductile materials were specified.

The axial stress (σ_z) expressed as a percentage of yield for each part is displayed in Figures 18 and 19, near the peak tension and peak compression loading. The black areas indicate compressive regions near yield, while the white areas indicate tensile regions near yield. Several regions reached the yield stress; for example, the dynamic model indicated stresses around yield and above the tape groove in the aluminum part and at the joint upset. Stressses just before the joint upset were not as high as calculated in the SASL model under static loading conditions. A similar plot normalizing the von Mises stress with the ultimate stress showed no regions near the ultimate material strength.

Deformations are also shown in Figures 18 and 19. In Figures 18.b and 19 the deformations indicated have been exaggerated by 2.5 times. (Also, the tape

joint assembly as shown is magnified—about 1.5 times for Figures 18.a and 19 and 2.5 times for Figure 18.b.) The rebound shock load passes through the tapes without significant deformation (or stress change). Only with displacement exaggeration and magnification can the tape rolling from the compressive rebound load be seen. The limited tape rolling for the wide tapes shown in Figure 18.b can be compared to the much greater tape rolling for the narrow tapes shown in Figure 8. The rebound load, however, does create a displacement wave in the stainless-steel case of about 10 kHz as discerned from Figures 19.a and 19.b.

In conclusion, the detailed computer model verified the tape joint dimensions developed using the simple design steps presented previously. (The reader should note the reason such a detailed analysis could be performed and the joint's behavior accurately predicted derived from the simple tape joint architecture.)

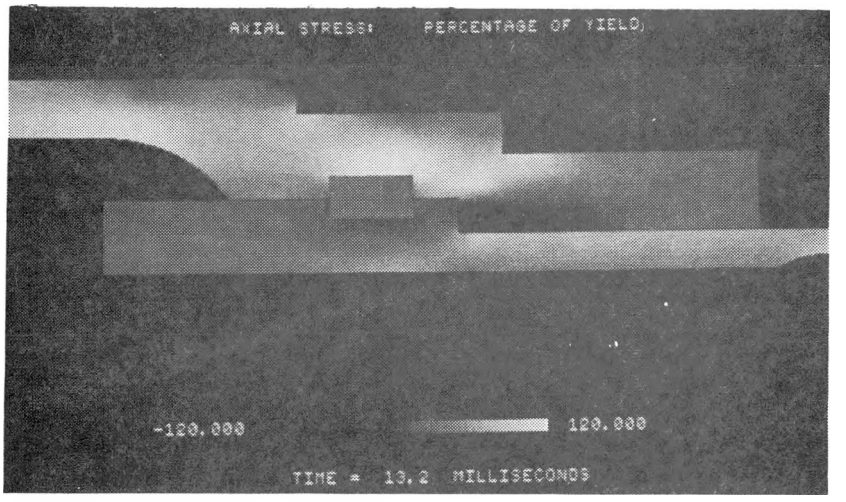

a. Overall view at peak tension

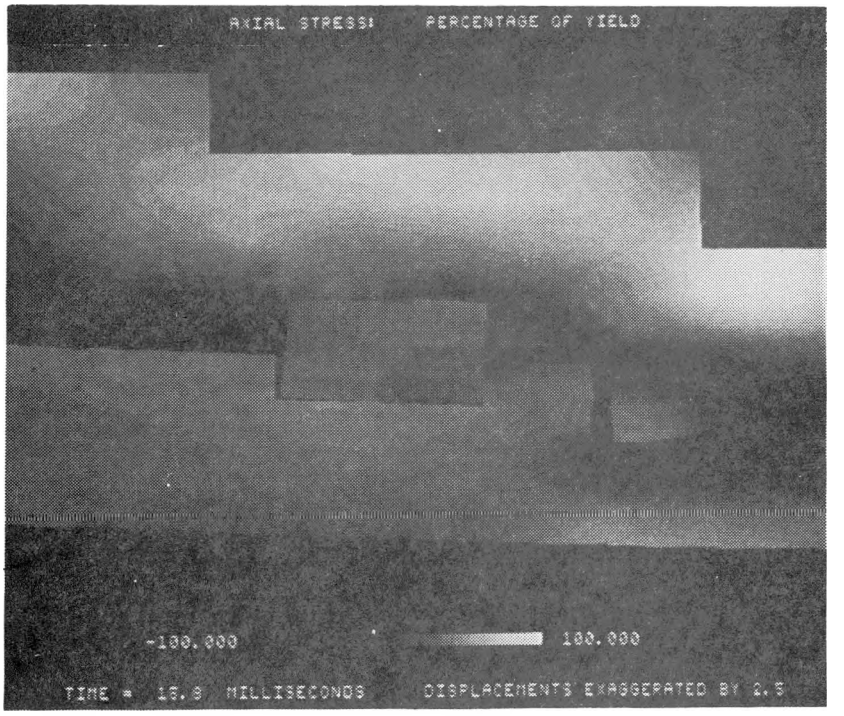

b. Closeup of tape region near peak compression

Figure 18. Stress Contours of Modified Joint

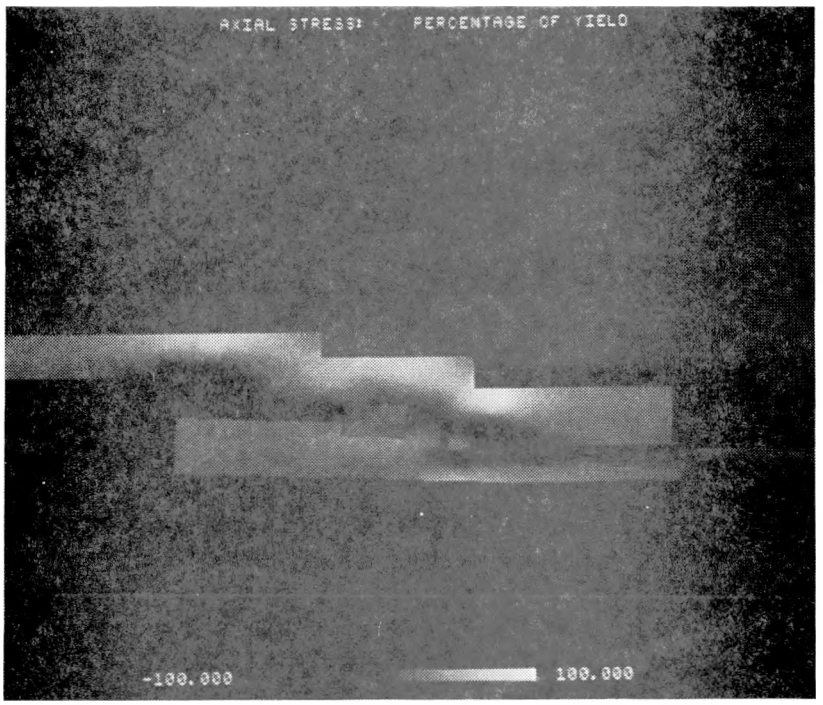

a. Time = 15.8 ms displacements exaggerated by 2.5

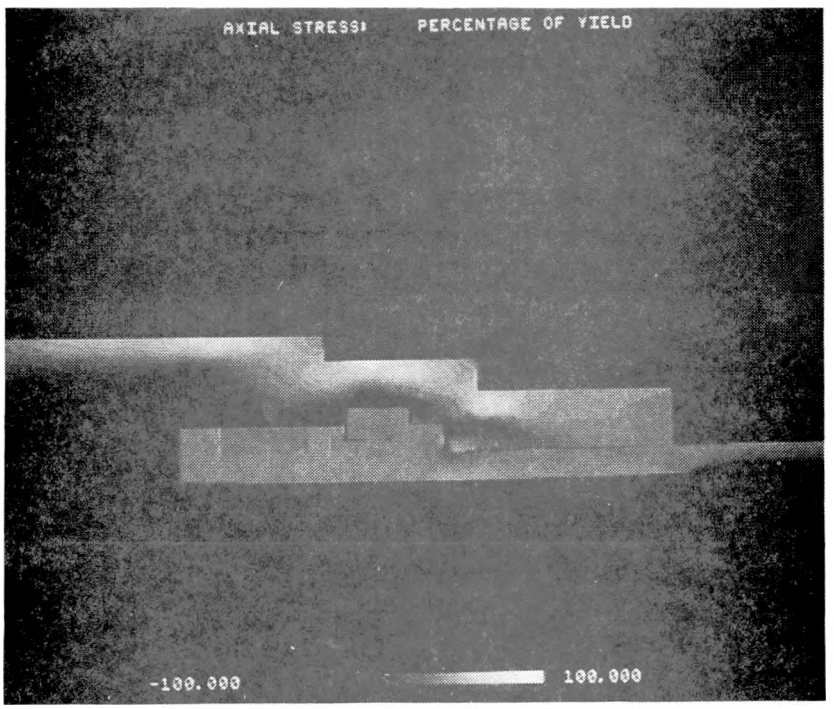

b. Time = 15.9 ms displacements exaggerated by 2.5

Figure 19. Stress Contours of Modified Tape Joint Showing Displacement Wave in Outer Stainless-Steel Case

Bibliography

Alvis, R. L., 1971, inventor, "Joint Utilizing Wedge-Shaped Rectangular Locking Shafts," US Patent No. 3600011, patent assigned to the Department of Energy.

"API Specification for Casing, Tubing, and Drill Pipe," 1976, American Petroleum Institute, Dallas, Texas.

Biffle, J. H., 1974, "SASL Computer Code Revision and Implementation," Informal Memorandum, Sandia Laboratories, Albuquerque, NM.

Blose, R. E., 1976, *A Study of the Mechanics of Tape Insertion and Resulting Assembly Forces in an Interlocking Tape Joint*, SAND75-0409 (Albuquerque, NM: Sandia Laboratories).

Fisher, J. W., and J. H. A. Struik, 1974, *Guide to Design Criteria for Bolted and Riveted Joints* (New York: John Wiley & Sons).

Hetenyi, M., 1946, *Beams on Elastic Foundation* (Ann Arbor, MI: The University of Michigan Press).

Huerta, M., and J. T. Black, 1976, *Experimental and Analytical Investigation of an Interlocking Tape Joint*, SAND76-0166 (Albuquerque, NM: Sandia Laboratories).

Hickerson, J., 1975, "Fatigue Notch Sensitivity of HP 9-4-20," Informal Memorandum, Sandia Laboratories, Albuquerque, NM.

Key, S. W., Z. E. Beisinger, and R. D. Krieg, 1978, *HONDO II: A Finite Element Computer Program for the Large Deformation Dynamic Response of Axisymmetric Solids*, SAND78-0422 (Albuquerque, NM: Sandia Laboratories).

Peterson, R. E., 1974, *Stress Concentration Factors* (New York: John Wiley & Sons).

Rolfe, S. T., and J. M. Barsom, 1977, *Fracture and Fatigue Control in Structures, Applications of Fracture Mechanics* (Englewood Cliffs, NJ: Prentice-Hall, Inc.).

DISTRIBUTION:

0311 W. A. Sebrell
1500 W. Herrmann
1510 D. B. Hayes
1520 D. J. McCloskey
1521 R. D. Krieg
1522 T. G. Priddy
1522 J. T. Black (15)
1522 S. D. Meyer (15)
1522 M. J. Sagartz
1523 R. C. Reuter
1523 R. A. May
1524 R. P. Rechard (15)
1524 W. N. Sullivan
1530 L. W. Davison
1540 W. C. Luth
5111 D. L. McCoy
5111 K. M. Timmerman (2)
5112 R. E. Howell
5112 R. S. Fox
8424 M. A. Pound
3141 L. J. Erickson (5)
3151 W. L. Garner (3)
3154-3 C. H. Dalin (25)
for DOE/TIC (Unlimited Release)